Current Biology, Vol. 12, 227–231, February 5, 2002, ©2002 Elsevier Science Ltd. All rights reserved. PII S0960-9822(02)00656-5

The *Drosophila* Standard Brain

Karlheinz Rein,[1,4,5] Malte Zöckler,[2,4] Michael T. Mader,[1,6] Cornelia Grübel,[1] and Martin Heisenberg[1,3]

[1] Lehrstuhl für Genetik und Neurobiologie
Biozentrum
Am Hubland
97074 Würzburg
Germany

[2] Konrad-Zuse-Zentrum für
Informationstechnik Berlin
Takustrasse 7
14195 Berlin
Germany

Summary

Organisms and organs come in sizes and shapes. With size, science has no problems, but how to quantify shape? How similar are two birds or two brains? This problem is particularly pressing in cases like brains where structure reflects function. The problem is not new, but satisfying solutions have yet to be worked out. For brain anatomy, no general methodology for a statistically secured quantitative description is available. Using the small brain of the fly *Drosophila melanogaster*, we have explored a new approach combining immunohistochemistry, high-resolution 3D confocal microscopy, and advanced graphics computing. For a genetic model organism such as *Drosophila,* a quantitative assessment of brain structure is particularly rewarding, since it allows for the identification of genetic variants with subtle brain structure phenotypes and, even more importantly, the organization of the wealth of gene expression patterns in the brain into a genetic atlas linking molecular and organismic gene function. We now provide a representative standard for the brain of *D. melanogaster* wild-type with means and variances for several aspects of its shape. Its application to volumetry, mutants, and gene expression patterns is demonstrated.

Results and Discussion

Generating the Standard Brain

For the human brain, significant efforts toward a more quantitative and statistical approach have been undertaken in the last decade (overview: [1]). For small brains, however, averages with variances do not exist as yet, although such mapping projects would face a vastly lower complexity. Especially for *Drosophila*, a standard for brain morphology would be an invaluable research tool. We therefore developed a new protocol that allowed us to generate high-resolution recordings of whole *Drosophila* brains using a monoclonal antibody (nc82) [2] that marks synaptic neuropil [3], but not the cellular cortex, fiber tracts, or glia (Figures 1A and 1B), all of which may be added later. Wild-type CantonS (CS) was chosen as the reference (Standard Brain), because it is widely used in behavioral and neurobiological studies.

Labeling

Data sets were visualized using commercial 3D imaging software (AMIRA, http://www.amiravis.com). In addition, each voxel was labeled to indicate the anatomical structure to which it belonged (Figure 1C). A total of 16 structures were chosen, comprising about 60% of the total neuropil (Figure 1D). The choice of these structures was a compromise between the detail of the resulting model and the amount of manual work required, as well as reliability in distinguishing neuropil regions. Optic lobes, the central complex, and mushroom bodies are easily labeled, being well circumscribed at all levels. Antennal lobes and lateral horns merge with the adjacent neuropil at some levels. For these structures, boundaries sometimes consist of changes in staining intensity or must be interpolated from previous and subsequent sections. Still, they can be reliably labeled, as documented by the standard deviations in Table 1.

Labeling is used for quantitative analysis such as volumetric measurements and for matching whole brains (registration), as well as for visualizing neuropil regions and deviations in their shape [4]. Specialized algorithms allow us to compute polygonal models of these structures (Figure 1D). They are much smaller data files than the original data sets (typically about 2 MB) and are therefore suitable for visualization on smaller computers and communication over the Internet [3].

Average volumes of the 16 neuropil areas from 28 CS females are shown in Table 1. Standard deviations lie around 15%. Note the good agreement between corresponding right and left structures. For the optic lobes, the absolute values can be compared to previous data obtained with similar methods [4]. For the medulla and the lobula, the absolute values are slightly larger; whereas, for the lobula plate, they exceed the earlier ones by 11%. This deviation can, at least in part, be attributed to a change in the embedding medium to which the lobula plate is exposed the most. (The new medium reduces shrinkage compared to that used in [4] [see the Experimental Procedures]).

Registration

Different image data sets have to be brought into a common coordinate system in order to be compared. Since brains have different shapes, choosing a certain structure as the origin will likely give suboptimal results because the alignment relies only on this one structure. Better results are obtained if each data set is aligned with a template data set comparing all available features. This procedure is called registration (for choice of template and other details, see the Experimental Procedures and the Supplementary Material available with this article online).

[3] Correspondence: heisenberg@biozentrum.uni-wuerzburg.de
[4] These authors contributed equally to this work.
[5] Present address: Tecan Proteomics, Feldkirchnerstrasse 12a, D-85551 München, Germany.
[6] Present address: Institute for Bioinformatics/MIPS, Ingolstaedter Landstraβe 1, 85764 Neuherberg/Munich, Germany.

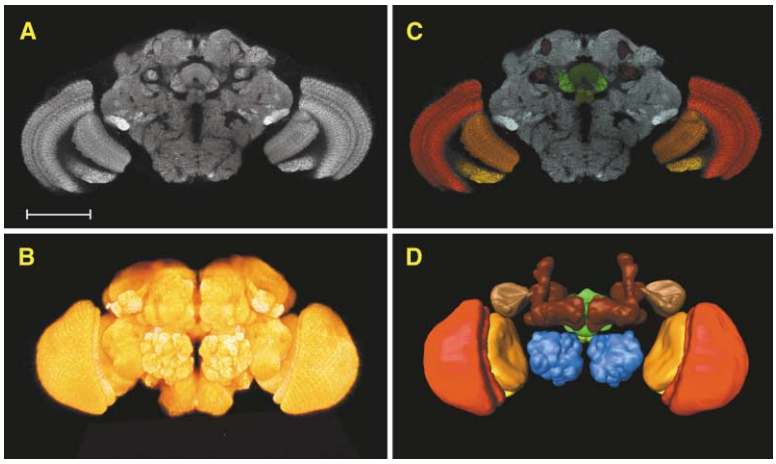

Figure 1. Four Visualization Procedures of Immunostained *Drosophila* Brain

(A) A virtual slice through the image data set in original recording orientation. Oblique frontal view (dorsal is more anterior). Note that laminae are missing, since the preparation leaves them with the eyes. The antigen has an elevated concentration in a small region of the lateral protocerebrum.

(B) 3D visualization of the image data by direct volume rendering and a color lookup table (red-yellow-white).

(C) Neuropil regions were manually labeled in all slices. The color code also applies to Figures 1D, 4A, and 4B). Red: medulla; orange: lobula; yellow: lobula plate; chocolate brown: mushroom body; beige: lateral horn (see Figure 1D); blue: antennal lobe (Figure 1D); olive green: noduli; dark green: ellipsoid body; light green: fan-shaped body; grayish green: protocerebral bridge (not visible in Figure 1D, as it is lying behind the fan-shaped body; but see Figure 4).

(D) A polygonal brain model generated from an individual labeled data set.

The scale bar represents 100 μm.

For the Standard Brain, only rigid and scaling transformations were applied. They compensate for differences in position, orientation, and size of the image data sets but preserve differences in shape and orientation as well as the relative location and size of the neuropil structures. Figure 2A shows an average intensity map in which 28 image data sets are superimposed. Comparison with a single data set (Figure 1A) gives an intuitive idea of the similarity of brains: the overlay still allows most of the structures to be recognized. In order to quantify the distribution of these structures in the overlay, an additional map was calculated (Figure 2D), indicating the probability for a labeled structure to occur at a particular voxel. Large structures like the optic lobe have large areas of overlap in all brains (dark red), whereas smaller structures such as the mushroom body α lobes have no region where all 28 of them overlap. To improve the registration, a scaling factor was introduced for each brain (Figures 2B and 2E). Note that the average intensity maps still have the original orientation of the template and are not rotated for optimal right-left symmetry.

For special applications, nonrigid registrations may be preferable and can provide an even better alignment of neuropil structures. For example, in Figures 2C and 2F, a rigid transformation was independently computed for each labeled structure. This yielded additional displacement vectors for labeled points. In order to generate a continuous displacement field for all points in the data set, a special interpolation algorithm was designed (see the Experimental Procedures). This procedure proved particularly useful for aligning enhancer GAL4 expression patterns to the Standard Brain that are double-stained for the reporter and synaptic neuropil (see below).

For many applications, the average intensity or probability maps will be the appropriate standard. In some cases, however, a representative single image data set may be preferable. This reference brain was defined as the data set that correlated best with the label average, which was obtained by calculating the probability that included the volume closest to the average volume for each structure in the probability map (see the Supplementary Material).

Table 1. Volumes of Neuropil Structures in the Standard Brain, CantonS Females

Structure	Volume (μ^3)	SEM	Standard Deviation (μ^3)
Medulla (r)	1.07^6	±2.8%	1.57^5
Medulla (l)	1.07^6	±2.4%	1.36^5
Lobula (r)	3.59^5	±2.9%	5.59^4
Lobula (l)	3.60^5	±2.8%	5.41^4
Lobula plate (r)	1.92^5	±3.7%	3.78^4
Lobula plate (l)	1.92^5	±3.4%	3.43^4
Mushroom body (r)	1.55^5	±3.4%	2.80^4
Mushroom body (l)	1.53^5	±3.3%	2.71^4
Ellipsoid body	3.56^4	±2.5%	4.62^3
Noduli	9.97^3	±3.1%	1.62^3
Fan-shaped body	1.04^5	±2.7%	1.49^4
Protocerebral bridge	1.98^4	±3.1%	3.20^3
Antennal lobe (r)	1.90^5	±2.6%	2.59^4
Antennal lobe (l)	1.91^5	±2.6%	2.58^4
Lateral horn (r)	8.40^4	±3.2%	1.44^4
Lateral horn (l)	8.83^4	±3.2%	1.48^4

Applications

Shape variability in a set of brains is evident in the average intensity map (Figure 2C). Two such maps of different sets can be superimposed on the screen to directly reveal group differences. For most applications, however, labeling substructures will be indispensable. Computing tools for this time-consuming step are continuously being improved.

Sexual Dimorphisms

Male and female brains were compared in two wild-type strains (Figure 3A), CantonS (CS) and Lindelbach (a village near Würzburg; WT-Li). In addition to the 28 CS females described above, 28 CS males as well as 33 females and 28 males of WT-Li were prepared from parallel cultures at the same time of the year. All image data sets were labeled and averaged. As reported earlier [4], females have larger medullae in accord with their larger number of facets and visual elements. In contrast, the lobula and lobula plate have the same size in the

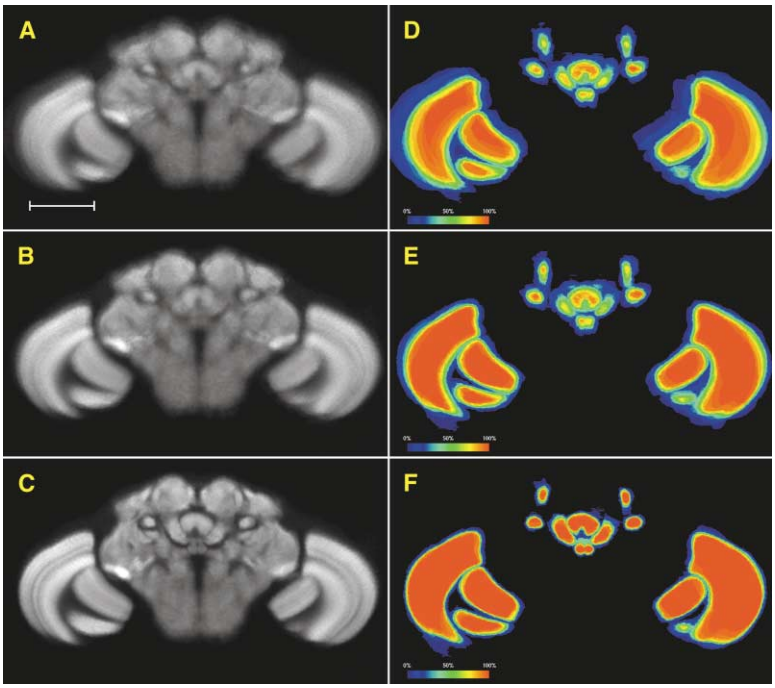

Figure 2. Average Intensity and Probability Maps

(A–C) One slice of the average intensity map for (A) rigid, (B) rigid and scaled, and (C) rigid, scaled, and per-structure registration.

(D–E) Respective probability maps for all labeled structures. The probability to find a structure at a particular position is color coded: red: 100%; black: 0%. Note that, in (D) and (E), the map indicates the variation of position and shape; in (F), only of shape.

The scale bar represents 100 μm.

two genders, despite the smaller number of projections from the eye in males, suggesting additional neuropil for male-specific processing in these neuropil regions. In the central brain, most structures are larger in females than in males. For the antennal lobe, the difference is about 9% for both strains, although a recent study [5] reported no sexual dimorphism in its glomerular pattern. In CS, the mushroom body and lateral horn also follow this pattern; whereas, in WT-Li, these structures show no significant sexual dimorphism.

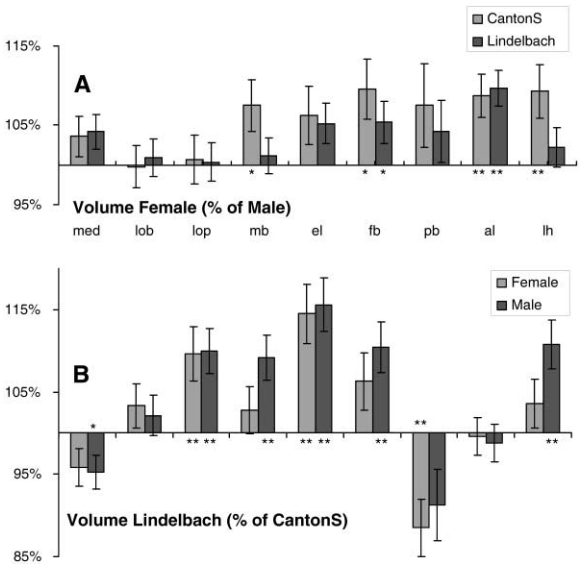

Figure 3. Relative Volume Differences between Neuropil Regions

(A) Females versus males (med: medulla; lob: lobula; lop: lobula plate; mb: mushroom body; el: ellipsoid boy; fb: fan-shaped body; pb: protocerebral bridge; al: antennal lobe; lh: lateral horn).

(B) CantonS versus Lindelbach (abbreviations are the same as in [A]).

Volume Differences between Wild-Types CantonS and Lindelbach

Comparison of these two lines may be interesting, as CS has been kept in food vials for well over 1000 generations, whereas WT-Li has been living in the laboratory since only 1992 (about 130 generations at the time of the experiment). The lobula plate, which is well known to serve visual flight control [6–8], is 10% larger in WT-Li than in CS, and the ellipsoid body, also tentatively associated with flight and visual processing [8, 9], is even 15% larger. In contrast, the protocerebral bridge, a premotor area for walking control[10, 11], is 10% larger in CS than in WT-Li. These differences suggest an adaptive trend from flight to walking in the food vials. Similarly, courtship under crowded laboratory conditions may have gradually affected the olfactory pathway in males, as their mushroom bodies and lateral horns are about 10% smaller in CS than in WT-Li.

A special advantage of average intensity and probability maps is that any shape differences that might underlie or accompany volume differences can be visualized and quantified (optic lobes: [4]). For instance, it would be interesting to know how the doughnut-shaped ellipsoid body is affected by the volume change. These results will be presented later (but, as an example, see “Mutants” below).

Mutants

Many *Drosophila* genes have been discovered in screens for aberrant brain structure [12–14]. They are normally referred to by the defect that led to their discovery. More subtle changes in other regions of the brain may remain undiscovered. To properly account for the effect of a particular mutation on brain structure, the genetic background of the mutant line has to be matched to that of the Standard Brain, and an average mutant brain has to be generated. In the present study, a 3D image of a single mutant brain is shown superim-

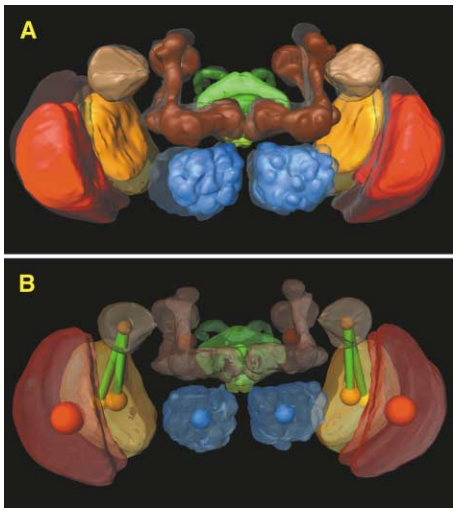

Figure 4. Brain Structure Mutant *reduced optic lobes*, *rol*

(A) Superimposed polygonal models of the representative CS brain (transparent) and arbitrarily chosen *rol* image data set. The *rol* data set was scaled using the average volume of only the labeled central brain structures. The color code is the same as that defined in Figure 1C.
(B) Spheres (same color code as in (A) and Figures 1C and 1D) show centers of gravity of labeled structures. Green bars indicate that distances between labeled structures are 3%–5% smaller than in CS flies.

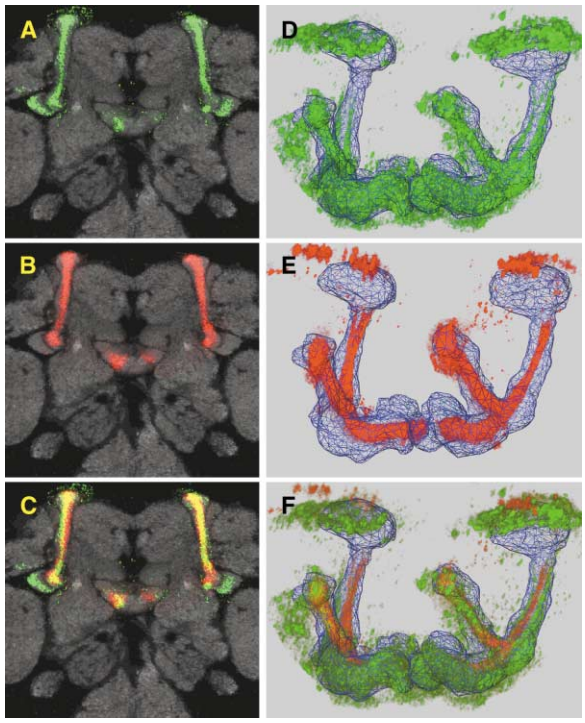

Figure 5. Two Enhancer GAL4 Lines with *lacZ* Reporter Gene Expression in the Mushroom Bodies

Brains are double stained with anti-β-Gal and nc82 antibodies and are aligned to the reference CS female brain using per-structure registration.
(A–C) The anti-β-Gal staining is shown together with the synaptic neuropil of the reference brain. (C) is a superposition of (A) and (B).
(D–E) The Kenyon cell fiber bundle is seen in a "wireframe" model of the mushroom body of the reference brain: (A and D) P[GAL4]-201y/UAS_{GAL4}-lacZ (green); (B and E) P[GAL4] 17d/UAS_{GAL4}-lacZ (red); (F) is a superposition of (D) and (E).

posed on the (transparent) Standard Brain (Figure 4A). This strain, *reduced optic lobes* (*rol*) [15], has, as its name suggests, a hypoplasia in the primary visual neuropil. In mass-histological preparations, this phenotype is not easy to score. When superimposed, the difference is obvious, although the genetic background of *rol* has not been "cantonized".

A preliminary evaluation of eight animals reveals that the hypoplasia compared to CS is largest for the lobula plate (39% ± 4%), which had not been scored at all, and smallest for the lobula (14% ± 5%). The central brain seems to be generally larger than in CS (ellipsoid body: 15% ± 7%). Whether this increase persists in a controlled genetic background remains to be investigated. In contrast to the overall size of the central brain, the protocerebral bridge turns out 19% ± 5% smaller than in CS. The handlebar-shaped rod has about the same length, suggesting the normal number of 16 subunits, but is thinner in the mutant (not shown in Figure 4A). In the inspection of slices, even a large relative change of about 35% as a volume effect can easily be missed if no special attention is paid to this structure.

In Figure 4B, the colored spheres indicate the centers of gravity of the labeled neuropil structures. Deviations in their distances between mutant and wild-type can be represented by color-coded bars connecting these spheres. The green of the bars connecting the lobula and lobula plate to the lateral horn indicates a reduction of 3%–5% in the mutant. As most other distances are distinctly larger in *rol* than in CS, this reduction is a salient feature, indicating that the optic lobes are shifted upward and backward relative to the central brain and the optic lobes of CS flies. It should be obvious from the pictures and this short description that an exhaustive account of the *rol* brain defects would be a major project scrutinizing the genetics, labeling, and alignment procedures. This is beyond the scope of the present report. Given the abundance of brain structure variants in mutant screens [12], we expect many genes to have mutant brain structure phenotypes. The Standard Brain will help to identify and characterize them.

Gene and Enhancer Expression Patterns

Since the advent of immunocytochemistry and enhancer trap techniques [16], gene expression patterns have started to revolutionize brain anatomy and behavior research in *Drosophila*. Their usefulness critically depends upon our knowledge of the spatial and temporal distribution of expression levels in the tissue. One of the purposes of the Standard Brain is to provide a common reference for the spatial analysis of these patterns. In Figure 5, single flies from two enhancer GAL4 lines (201y and 17d) with expression in parts of the mushroom bodies are shown in the background staining (A–C) or mushroom body outline (D–F, blue) of the reference brain. Note the partial overlap (yellow) of the two sets of Kenyon cell fibers in these two lines. In 17d, about 425 fibers of the α/β lobes, and, in 201y, about 620 fibers predominantly of the γ lobe, but also of the α/β lobes, are marked [17].

We propose that laboratories characterizing gene expression patterns in the adult *Drosophila* brain use double labeling with nc82 and the same representative brain (Standard Brain) for registration. This quantitative approach will lead to a convergence of neuroanatomical data from different sources and result in a new type of atlas (database) combining structural, developmental, and molecular information.

The procedures presented here can also be applied to the *Drosophila* larval brain and to other insects like honeybee, where a Standard Brain is already being developed [18] and a single data set as a reference for Ca imaging in the antennal lobe [18] is in use. Moreover, the general approach is not restricted to brains. Any complex biological shapes such as embryos or organs (e.g., leaves, kidneys, shells) could be quantified in this way.

Experimental Procedures

Flies, Preparation, Histology, and Microscopy

Whole adult *Drosophila* brains were dissected from 5-day-old flies raised under controlled rearing conditions (e.g., light, temperature, larval density). Intact brains were fixed overnight in 2% paraformaldehyde at 4°C. The neuropil was stained with the monoclonal antibody nc82 against synaptic protein [2] and a secondary antibody conjugated with CY3.18 (Jackson Immuno Research). Vectashield was used for embedding. To reduce shrinkage, it was diluted with glycerol (3:1). Optical sections were acquired using a Leica TCS confocal microscope equipped with a Leica 20× lens with a numerical aperture of 0.7. Resolutions were about 1 μm horizontally and about 2 μm axially.

Data Handling and Visualization

A typical data set consists of 1024 × 1024 × 200 voxels with 8-bit intensity resolution corresponding to a size of about 200 MB. The voxel size of a data set is 0.6 × 0.6 × 1.1 μm after correcting for diffraction index mismatch. We have used the visualization software AMIRA (www.amiravis.com) on several SGI Onyx2 and Onyx3 systems and on standard graphic PCs for visualization, segmentation, and data processing. Special purpose algorithms were implemented as custom AMIRA scripts and modules.

Template and Registration

The template was chosen as the data set with the most average volume for each substructure. Different methods for registration were investigated, including gray value correlation, label correlation, and minimization of distances of centers of gravity for individual structures. For the Standard Brain, we have chosen the label correlation, because it takes into account the additional anatomical information from the labeling, yielding a very robust registration. A uniform scaling factor was determined from volume ratios.

Nonrigid Registration

After computing the global rigid transformation, individual rigid transformations are computed for each labeled structure (see above Registration) and interpolated using partial differential equations to generate a continuous displacement. A wide variety of different methods for elastic registrations have been proposed for different applications, including landmark-based methods, optical flow-based methods, free-form deformations, or mechanical simulations [1]. In general, it is not easy to understand the meaning of correspondence of two points under an elastic transformation, since the elastic transformation may eliminate preparation artifacts like mechanical deformations as well as anatomical variability.

Software and Resulting Data

The specific modules used for this project as well as the resulting brain models are made available at http://www.amiravis.com/vib and described in the Supplementary Material and [19].

Supplementary Material

Supplementary Material including details about the individual steps of the data processing pipeline and the specific algorithms used is available at http://images.cellpress.com/supmat/supmatin.htm.

Acknowledgments

We thank A. Valaas for language editing.

Received: October 10, 2001
Revised: December 12, 2001
Accepted: December 12, 2001
Published: February 5, 2002

References

1. Toga, A.W. (2001). Maps of the brain. Anat. Rec. *265*, 37–53.
2. Hofbauer, A. (2000). Eine Bibiliothek monoklonaler Antikörper gegen das Gehirn von *Drosophila melanogaster*. Habilitation thesis, Würzburg University, Würzburg, Germany.
3. Rein, K., Hiesinger, P., Zöckler, M., Kirsten, J., Fischbach, K.-F., and Heisenberg, M. (2000). Three-dimensional reconstruction of the *Drosophila* larval and adult brain. Flybrain (http://www.flybrain.org).
4. Rein, K., Zöckler, M., and Heisenberg, M. (1999). A quantitative three-dimensional model of the *Drosophila* optic lobes. Curr. Biol. *9*, 93–96.
5. Laissue, P.P., Reiter, C., Hiesinger, P.R., Halter, S., Fischbach, K.-F., and Stocker, R.F. (1999). Three-dimensional reconstruction of the antennal lobe in *Drosophila melanogaster*. J. Comp. Neurol. *495*, 543–552.
6. Hausen, K. (1981). Monocular and binocular computation of motion in the lobula plate of the fly. *Verh. dt. Zool. Ges.* 49–70.
7. Blondeau, J. (1981). Electrically evoked course control in the fly *Calliphora erythrocephala*. J. Exp. Biol. *92*, 143–153.
8. Borst, A., and Egelhaaf, M. (1989). Principles of visual motion detection. Trends Neurosci. *12*, 298–306.
9. Bausenwein, B., Müller, N.R., and Heisenberg, M. (1994). Behavior-dependent activity labeling in the central complex of *Drosophila* during controlled visual stimulation. J. Comp. Neurol. *340*, 255–268.
10. Hanesch, U., Fischbach, K.-F., and Heisenberg, M. (1989). Neuronal architecture of the central complex in *Drosophila melanogaster.* Cell Tissue Res. *257*, 343–366.
11. Strauss, R., and Heisenberg, M. (1993). A higher control center of locomotor behavior in the *Drosophila* brain. J. Neurosci. *13*, 1852–1861.
12. Heisenberg, M., and Böhl, K. (1979). Isolation of anatomical brain mutants of *Drosophila* by histological means. Z. Naturforsch. [C] *34c*, 143–147.
13. deBelle, J.S., and Heisenberg, M. (1996). Expression of *Drosophila* mushroom body mutations in alternative genetic backgrounds: a case study of the mushroom body miniature gene (mbm). Proc. Natl. Acad. Sci. USA *93*, 9875–9880.
14. Heisenberg, M., Borst, A., Wagner, S., and Byers, D. (1985). *Drosophila* mushroom body mutants are deficient in olfactory learning. J. Neurogenet. *2*, 1–30.
15. Heisenberg, M., and Wolf, R. (1984). Vision in *Drosophila*. Genetics of Microbehavior (Berlin: Springer).
16. O'Kane, C.J., and Gehring, W.J. (1987). Detection in situ of genomic regulatory elements in *Drosophila*. Proc. Natl. Acad. Sci. USA *84*, 9123–9127.
17. Mader, M.T. (2001). Analyse von Expressionsmustern in den Pilzkörpern von *Drosophila melanogaster*. Diploma thesis, Würzburg University, Würzburg, Germany.
18. Galizia, C.G., McIlwrath, S.L., and Menzel, R. (1999). A digital 3D atlas of the honeybee antennal lobe based on optical sections acquired using confocal microscopy. Cell Tissue Res. *295*, 383–394.
19. Zöckler, M., Rein, K., Stalling, D., Brandt, R., and Hege, H.-C. (2001). Creating virtual insect brains with Amira. Zuse Institut Berlin, in press.